

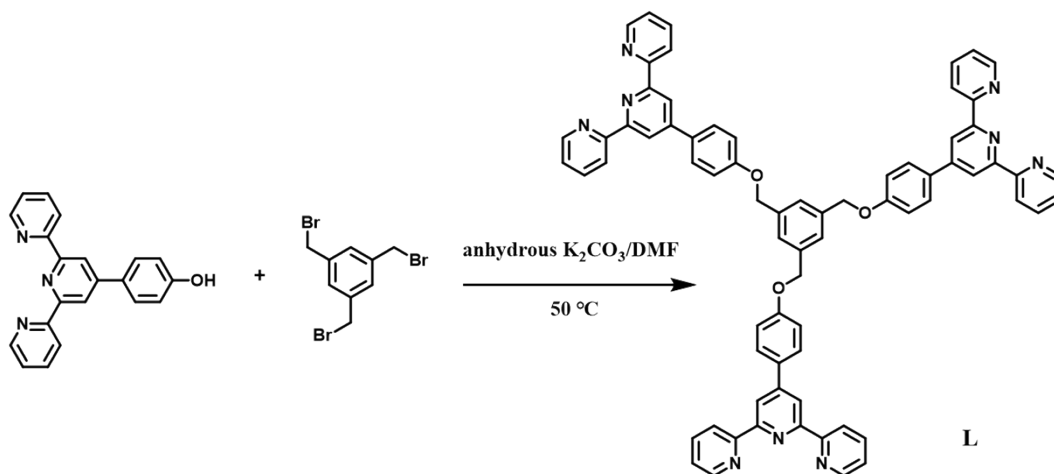
Supporting information

Interfacial self-assembly of a rigid-flexible terpyridine-Fe(II) supramolecular film and the electrochromic performance of its solid-state devices

Xiaomeng Sun, Xinfeng Cheng,* Xiya Chen, Hongwei Wang, Qian Zhao, Chunxia Yang, Xianchao Du, Xiaojing Xing, and Dongfang Qiu*

College of Chemistry and Pharmaceutical Engineering, Nanyang Normal University, Nanyang 473061, China

* Correspondence: x.f.cheng@nynu.edu.cn (X.C.); qiudf2008@nynu.edu.cn (D.Q.)



Scheme S1. Synthetic process of the target ligand **L**

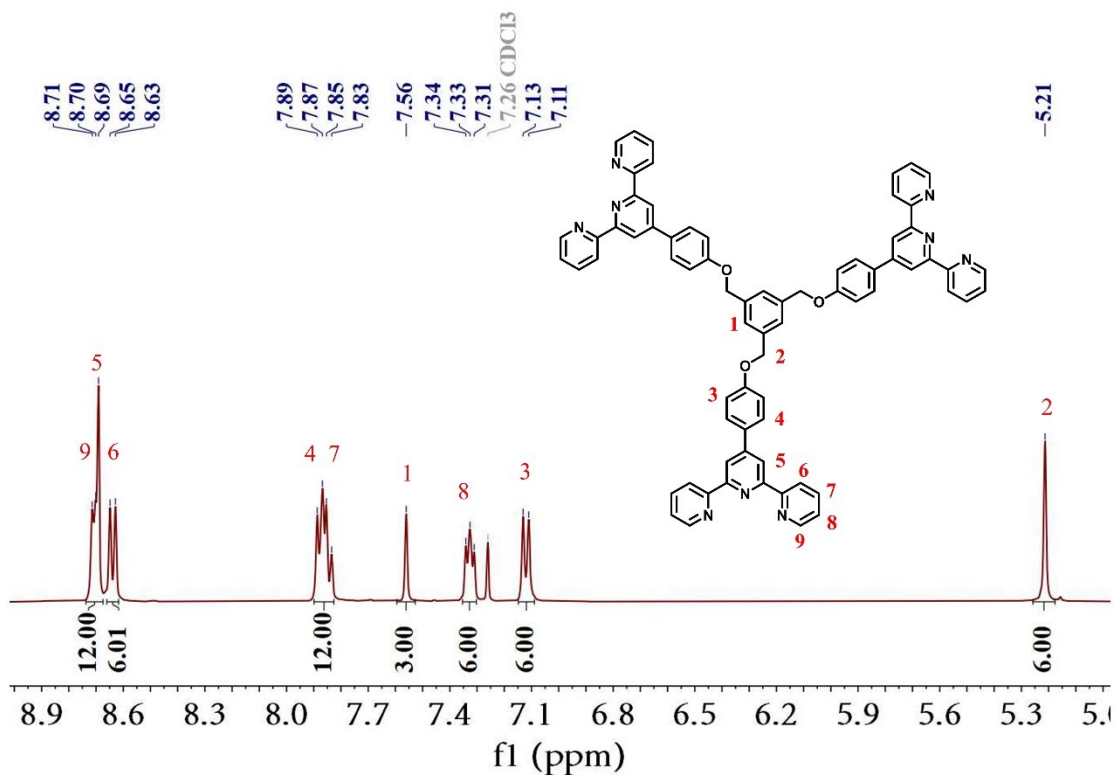


Figure S1. ^1H NMR spectrum of **L** (400 MHz, $CDCl_3$)

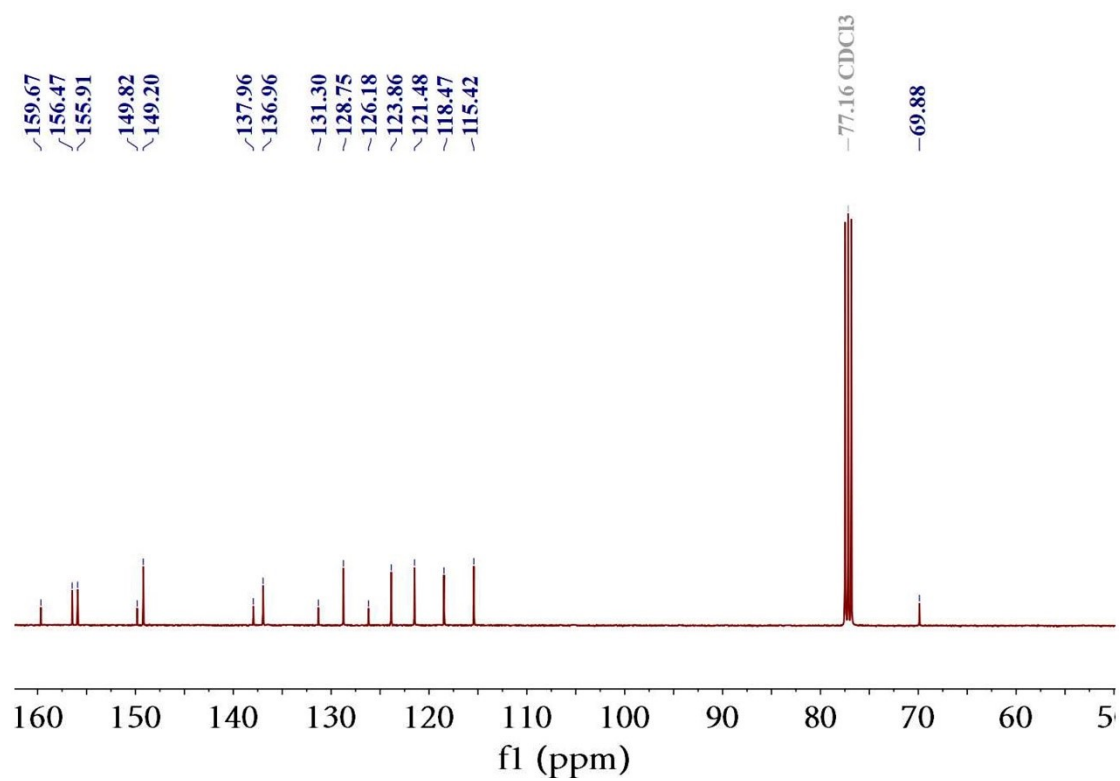


Figure S2. ^{13}C NMR spectrum of **L** (100 MHz, CDCl_3)

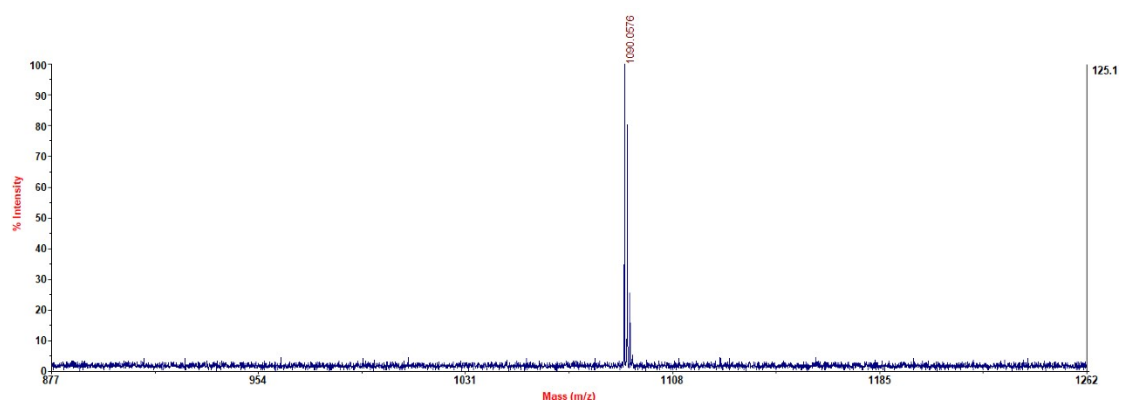


Figure S3. MALDI-TOF spectrum of **L**

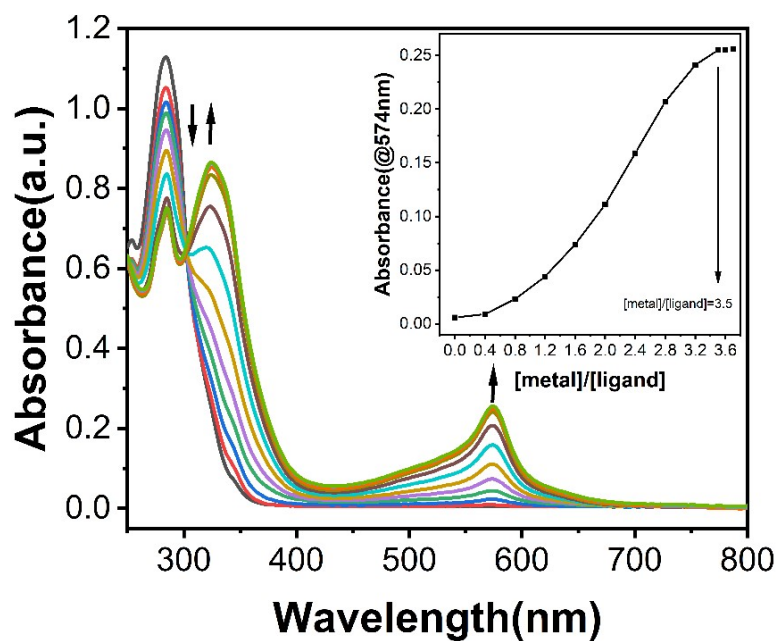







Figure S4. UV-vis absorption spectrum changes of the target ligand (10^{-5} M) in CH_3CN solution by continuous titration of FeSO_4 aqueous solution (10^{-3} M). Inset: The absorbance value at $\lambda_{\text{max, abs}} = 574$ nm changes with the concentration ratio of Fe^{2+} and ligand **L**.

Table S1. Images of the **L-Fe** film coated ITO glasses obtained by self-assembly of various concentrations of **L** in CH_2Cl_2 solutions and absorbance values at $\lambda_{\text{max, abs}} = 574$ nm.

Ligand concentration	10^{-3}M	$5 \times 10^{-4}\text{M}$	10^{-4}M	$5 \times 10^{-5}\text{M}$	10^{-5}M
film					
Abs@574nm	0.87	0.575	0.194	0.147	0.054

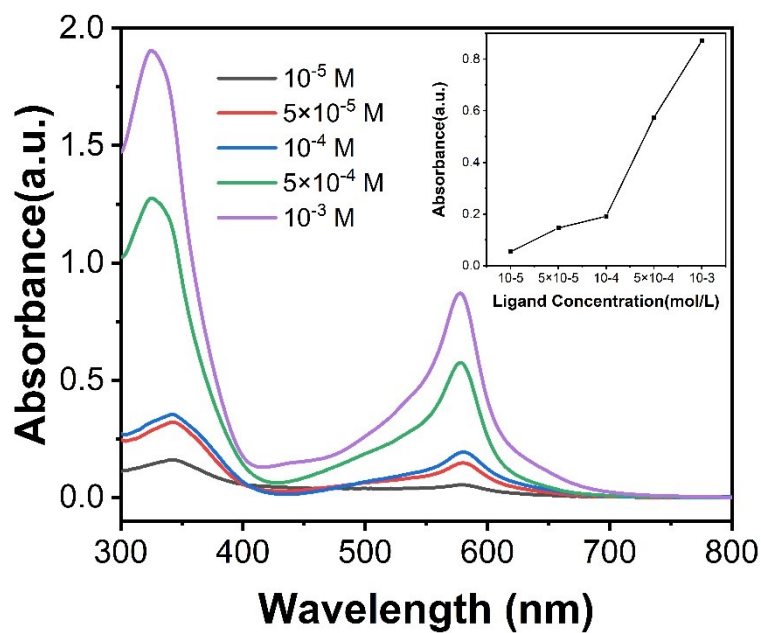


Figure S5. UV-vis absorption spectra of the **L-Fe** film coated ITO glasses obtained by self-assembly of various concentrations of **L** in CH_2Cl_2 solutions. Inset: Absorbance value at $\lambda_{\text{max, abs}} = 574 \text{ nm}$ changes with the concentration of **L** in CH_2Cl_2 solution.

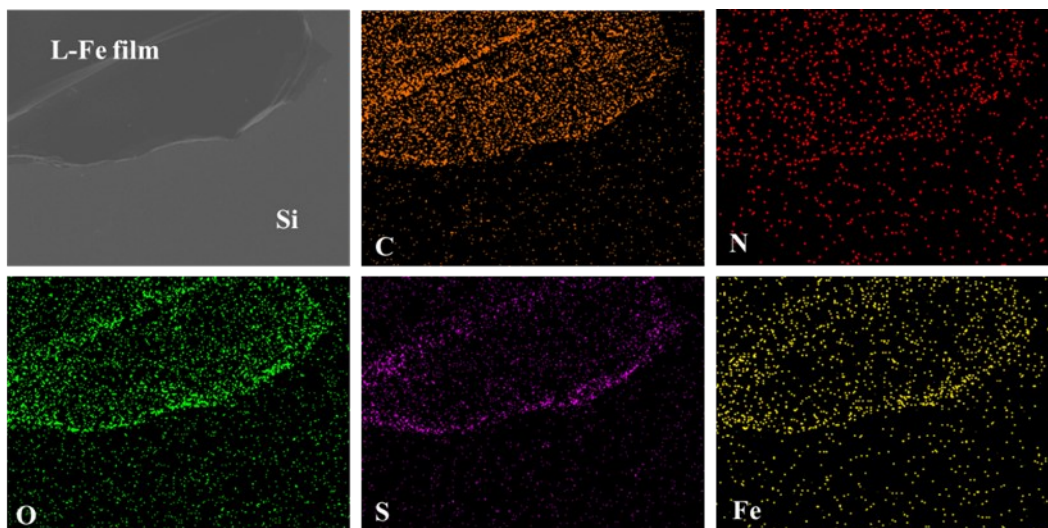


Figure S6. SEM and SEM/EDS element mapping images of the **L-Fe** film deposited Si substrate.

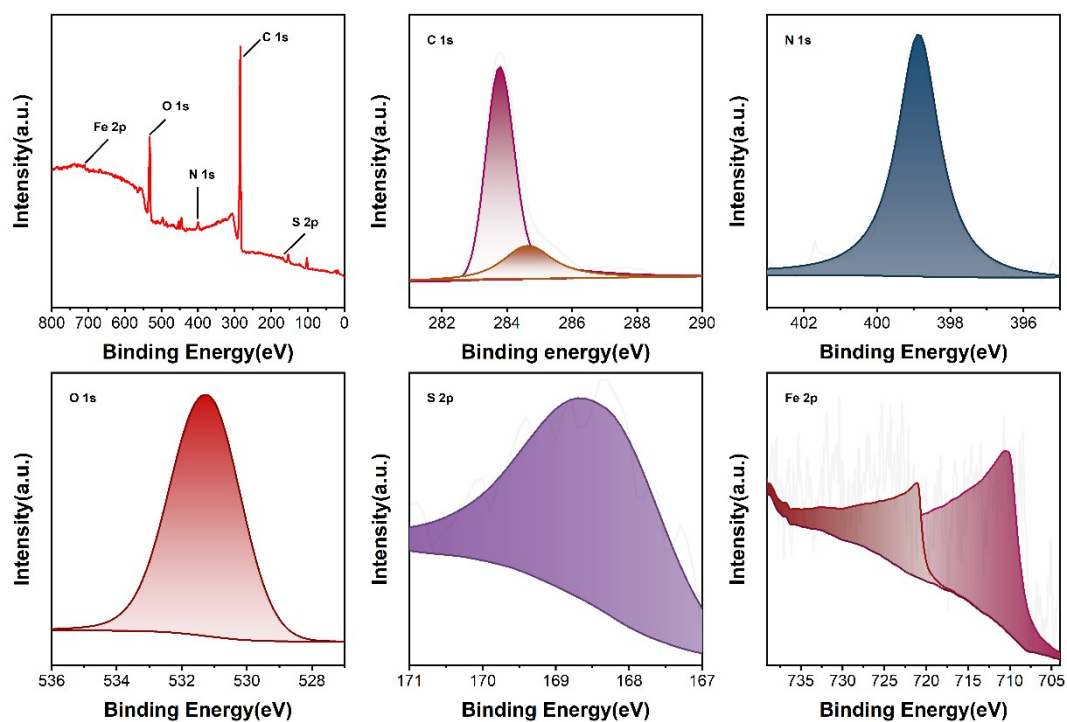


Figure S7. Full and fine XPS spectra of the **L-Fe** CONASHs film deposited Si substrate.

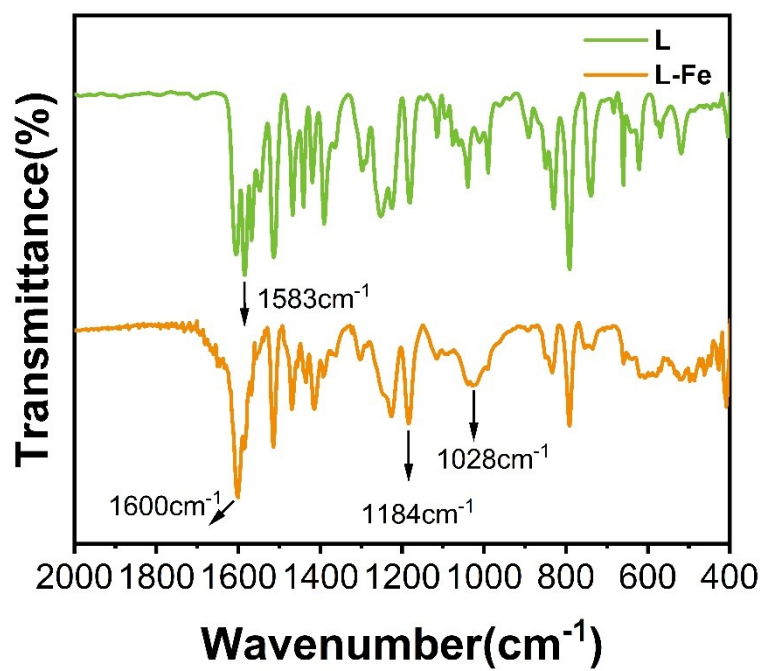


Figure S8. FT-IR spectra of **L** and **L-Fe** CONASHs film.

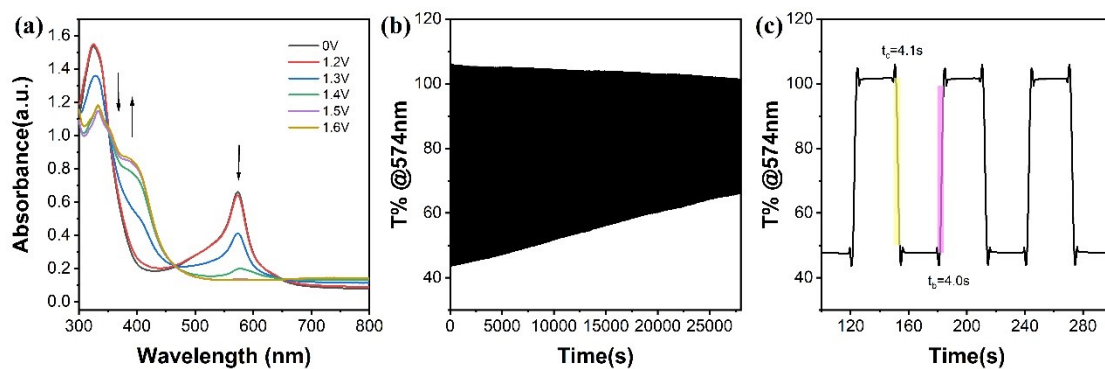


Figure S9. (a) Spectroelectrochemical properties of the **L-Fe** CONASHs film in 0.1 M $n\text{Bu}_4\text{NClO}_4/\text{CH}_3\text{CN}$ electrolyte solution. (b) Transmittance change at $\lambda_{\text{max, abs}} = 574$ nm upon applying the switch voltages between 0 and +1.5 V with a pulse width of 30 s. (c) Coloring and bleaching times of **L-Fe** CONASHs film.

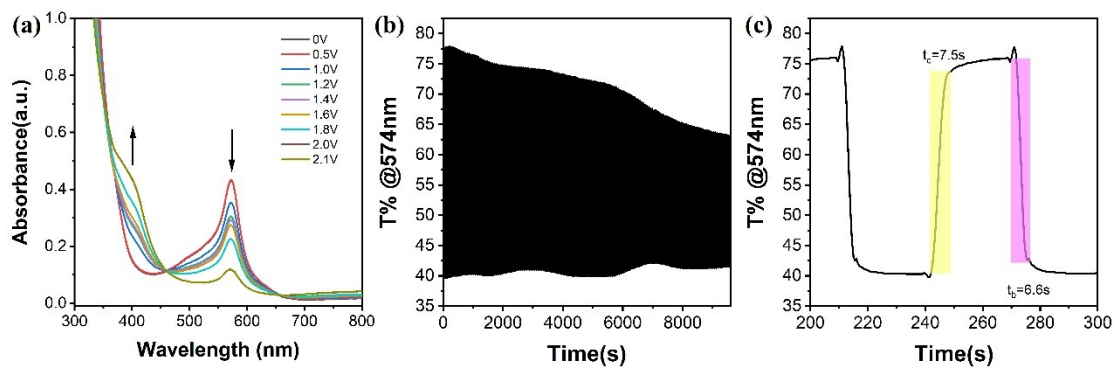
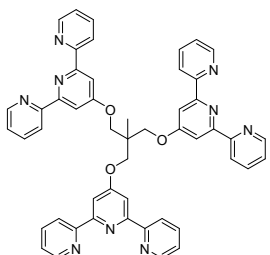
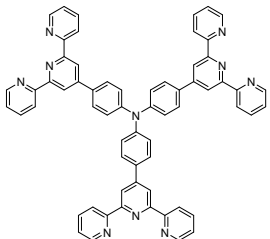
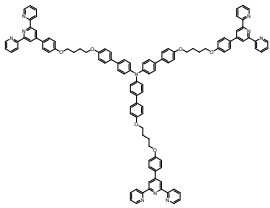
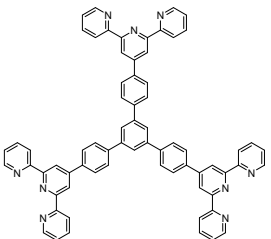
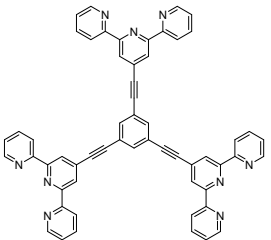
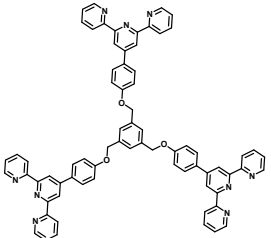


Figure S10. (a) Spectroelectrochemical behavior of the large-area **L-Fe** solid-state device (7×7 cm^2). (b) Long-term stability of the large-area device at $\lambda_{\text{max, abs}} = 574$ nm upon applying the switching voltages between -0.8 and +2.1 V with a pulse width of 30 s. (c) Coloring and bleaching times of the large-area device.

Table S2. Electrochromic performance of the three-arm TPY based CONASHs devices reported previously and in this paper.

Ligand Structure	Metal ions	ECD type	EC performance							Reference	
			λ_{\max} (nm)	Color Change	Coloration Step		Bleaching Step		ΔT_{\max} (%)		Long-term stability
					Response time (s)	CE (C ⁻¹ ·cm ²)	Response time (s)	CE (C ⁻¹ ·cm ²)			
	Fe(II)	Liquid	556	Intense pink/colorless	0.84	-	0.88	-	-	-	34
		Solid			1.15	470.16	2.49	-	53	1000	
	Fe(II)	Liquid	580	purplish red /orange-yellow /green	0.5	141.72	0.4	-	22.3	500	36
		Solid			1	-	0.9	-	-	-	
	Fe(II)	Liquid	570	Purple/yellow-green	14.3	172.82	7.3	-	20	-	31

	Fe(II)	Liquid	578	deep purple / pale yellow	-	-	-	-	-	800	30
		Solid	579		-	-	-	-	-	-	
	Fe(II)	Liquid	588	deep violet/ pale yellow	0.54	-	-	-	-	1000	
	Fe(II)	Liquid	574	purple/pa le yellow	4.1	581.0	4.0	233.7	53.9	500	This work
		Solid	574		3.9	875.2	3.7	182.3	56.3	500	